REPORT

A Homozygous Mutation in *KCTD7* Links Neuronal Ceroid Lipofuscinosis to the Ubiquitin-Proteasome System

John F. Staropoli,[1,2] Amel Karaa,[1] Elaine T. Lim,[1,3] Andrew Kirby,[1,3,4] Naser Elbalalesy,[5] Stephen G. Romansky,[6] Karen B. Leydiker,[7] Scott H. Coppel,[1] Rosemary Barone,[1] Winnie Xin,[1,8] Marcy E. MacDonald,[1,8] Jose E. Abdenur,[7] Mark J. Daly,[1,3,4] Katherine B. Sims,[1,8] and Susan L. Cotman[1,8,*]

Neuronal ceroid lipofuscinosis (NCL) is a genetically heterogeneous group of lysosomal diseases that collectively compose the most common Mendelian form of childhood-onset neurodegeneration. It is estimated that ~8% of individuals diagnosed with NCL by conservative clinical and histopathologic criteria have been ruled out for mutations in the nine known NCL-associated genes, suggesting that additional genes remain unidentified. To further understand the genetic underpinnings of the NCLs, we performed whole-exome sequencing on DNA samples from a Mexican family affected by a molecularly undefined form of NCL characterized by infantile-onset progressive myoclonic epilepsy (PME), vision loss, cognitive and motor regression, premature death, and prominent NCL-type storage material. Using a recessive model to filter the identified variants, we found a single homozygous variant, c.550C>T in *KCTD7*, that causes a p.Arg184Cys missense change in potassium channel tetramerization domain-containing protein 7 (KCTD7) in the affected individuals. The mutation was predicted to be deleterious and was absent in over 6,000 controls. The identified variant altered the localization pattern of KCTD7 and abrogated interaction with cullin-3, a ubiquitin-ligase component and known KCTD7 interactor. Intriguingly, murine cerebellar cells derived from a juvenile NCL model (CLN3) showed enrichment of endogenous KCTD7. Whereas *KCTD7* mutations have previously been linked to PME without lysosomal storage, this study clearly demonstrates that *KCTD7* mutations also cause a rare, infantile-onset NCL subtype designated as CLN14.

Neuronal ceroid lipofuscinosis (NCL) comprises a group of at least nine distinct and currently untreatable lysosomal storage diseases with overlapping clinical features, including progressive motor and cognitive decline, pigmentary retinal degeneration and vision loss in most cases, seizures, movement disorder, and eventual premature death.[1] NCL is estimated to have a worldwide prevalence of 1:100,000 individuals, and there is higher prevalence in some geographic regions.[1] Most forms of NCL are autosomal recessive and show autofluorescent lysosomal storage material with distinctive ultrastructural morphology in many cell types. At least nine genes have been implicated in the pathogenesis of NCL: *PPT1* (*CLN1* [MIM 600722]), *TPP1* (*CLN2* [MIM 607998]), *CLN3* (MIM 607042), *CLN5* (MIM 608102), *CLN6* (MIM 606725), *MFSD8* (*CLN7* [MIM 611124]), *CLN8* (MIM 607837), *CTSD* (*CLN10* [MIM 116840]),[2] and *DNAJC5* (*CLN4*; autosomal-dominant Kufs disease or late-onset NCL [MIM 611203]).[3,4] Despite the discovery of over 365 NCL-causing mutations in these genes, many clinically suspected cases of NCL remain molecularly undefined,[5] and these include ~8% of probands enrolled in the Massachusetts General Hospital (MGH) NCL Registry. With the aim of identifying novel causes of NCL, we focused our efforts on samples from a family with more than one affected member with strong clinical and histopathological evidence of NCL (Figure 1). We report the results of whole-exome sequencing and functional studies to identify the gene defect in this family, in which screening of the defined NCL-associated genes failed to identify known or predicted deleterious variants.

Medical history from several individuals in a Mexican family whose ancestors originated from the state of Michoacán was reviewed, and DNA samples were obtained after all subjects or legal guardians gave informed consent as required by the institutional review board at MGH. Both affected siblings (IV-1 and IV-2, Figure 2A) had a normal birth and infancy and suffered from seizures manifesting at 9 (IV-1) and 8 (IV-2) months of age. Seizure manifestations, confirmed by electroencephalography and video telemetry, included frequent myoclonic movements involving mainly the face and extremities, were often precipitated or worsened by fevers, and were refractory to multiple antiepileptic drugs. Normal developmental milestones were documented until the age of approximately 18 months, at which point motor and speech regression were noted. By the ages of 12 years (IV-1) and 10 years (IV-2), both siblings had microcephaly, were nonverbal, and were without spontaneous motoric function. Both IV-1 and IV-2 showed no response to visual threat and had markedly diminished pupillary light reflexes; in addition, IV-2 showed mild bilateral optic atrophy without

[1]Center for Human Genetic Research, Massachusetts General Hospital, Boston, MA 02114, USA; [2]Department of Pathology, Massachusetts General Hospital, Boston, MA 02114, USA; [3]Analytic and Translational Genetics Unit, Department of Medicine, Massachusetts General Hospital, Boston, MA 02114, USA; [4]Broad Institute of Harvard and MIT, Cambridge, MA 02142, USA; [5]Division of Neurology, Children's Hospital of Orange County, Orange, CA 92868, USA; [6]Pediatric Pathology, Miller Children's Hospital, Long Beach, CA 90806, USA; [7]Division of Metabolic Disorders, Children's Hospital of Orange County, Orange, CA 92868, USA; [8]Department of Neurology, Massachusetts General Hospital, Boston, MA 02114, USA
*Correspondence: cotman@helix.mgh.harvard.edu
http://dx.doi.org/10.1016/j.ajhg.2012.05.023.

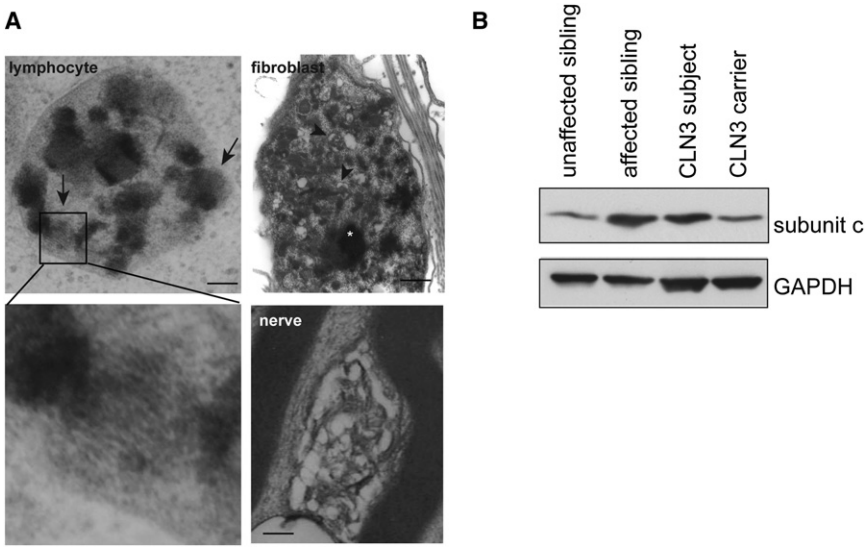

Figure 1. Storage Material in a Molecularly Undefined Form of NCL

(A) Electron micrographs demonstrating osmiophilic, membrane-bound storage material from peripheral blood (left panels) and a skin biopsy (right panels) from the proband. Arrows point to laminated inclusions, consistent with fingerprint profiles, in a lymphocyte. The upper right panel shows a fibroblast distended with a mixture of granular osmiophilic deposits (asterisk) and filamentous material, some of which is enclosed in vacuoles (arrowheads). The lower right panel shows a vacuole containing rectilinear profiles within the axon of a myelinated nerve. Scale bars represent 100 nm (lymphocyte), 500 nm (fibroblast), and 200 nm (nerve).

(B) Early-passage ($p < 3$) lymphoblastoid cell lines were established from an affected and unaffected sibling in the family studied here, as well as from a JNCL subject homozygous for a nonsense change (p.Tyr199*) in CLN3 and from an unaffected sibling heterozygous for the same CLN3 change. Lysates (~30 μg) were probed for mitochondrial ATPase subunit c, the protein characteristically stored in NCL. GAPDH served as a loading control.

apparent retinopathy. Brain imaging in both probands showed global cortical atrophy, particularly marked in the cerebellum, as well as thinning of the corpus callosum and some loss of subcortical white matter in IV-1. Comprehensive metabolic testing of plasma, urine, and cerebrospinal fluid was normal in both siblings. A skin biopsy performed on IV-2 for clinical diagnostic purposes at 11 years of age revealed prominent NCL-type storage material in fibroblasts, neurons, and eccrine secretory epithelial cells. Electron microscopy of a clinical buffy coat sample from IV-2 was also remarkable for lysosomal storage material containing fingerprint-like profiles and granular osmiophilic deposits in ~15% of the analyzed lymphocytes (Figure 1A). Moreover, immunoblot analysis probing for subunit c of the mitochondrial ATP synthase, the main stored proteolipid in most forms of NCL with fingerprint, rectilinear, and curvilinear storage profiles, revealed that the affected sibling had higher levels of subunit c in a lymphoblastoid cell line than did the unaffected sibling. This was similar to what was seen in a lymphoblastoid cell line from a juvenile NCL (JNCL) subject with a homozygous nonsense change in CLN3 (Figure 1B). Full sequencing of exons and flanking regions for all known genes associated with autosomal-recessive NCL (*PPT1*, *TPP1*, *CLN3*, *CLN5*, *CLN6*, *MFSD8*, *CLN8*, and *CTSD*) identified no known or predicted pathogenic mutations. Molecular analysis of genes associated with seizure disorders (*CDKL5*, *MECP2*, *SCN1A*, *SCN1B*), progressive myoclonic epilepsy (*EPM2A*, *EPM2B*, *EFHC1*, *CSTB*, and dodecamer repeat expansion in *CSTB*), and mitochondrial disease (including *POLG1* mutations and mutations associated with MELAS, MERRF, NARP, LHON, KSS, and CPEO) were unrevealing. Peripheral-blood lymphocytes from IV-2 were cytogenetically normal. Large genomic deletions, duplications, and insertions were ruled out on subjects IV-1 and IV-2 by array-based comparative genomic hybridization with an Agilent SurePrint G3 Human 4x180K microarray (MGH Diagnostic Molecular Pathology Laboratory, Boston, MA). Both siblings died from complications of progressive disease in their mid teens but showed no apparent extra-CNS disease. A third sibling in this family (IV-3) remains asymptomatic at age 7.

To identify a potential causative mutation in this family, we performed whole-exome capture and sequencing by using a NimbleGen SeqCap EZ Human Exome Library v.2.0 (Otogenetics Corporation; Norcross, GA) on samples from the two affected siblings (IV-1 and IV-2) and the unaffected sibling (IV-3, Figure 2A). The average coverage across each targeted exome was >50×, and >95% of all known SNPs were detected. The raw sequence data was processed through the variant-calling pipeline at the Broad Institute.[6,7]

Because the pattern of inheritance in this family was most likely autosomal recessive, we screened the sequence data for all pairs of homozygous and compound-heterozygous nonsynonymous (i.e., nonsense, splice site, read-through, missense, and indel) variants that were shared in the two affected siblings (IV-1 and IV-2), but not in the unaffected sibling (IV-3, Figure 2A). We required the variants to be present at ≤0.1% minor allele frequency in a set of 5,400 controls from the Exome Variant Server (National Heart, Lung, and Blood Institute [NHLBI] Exome Sequencing Project, Seattle, WA) given that the frequency of the most common known NCL-associated point and indel variants[2] in this dataset is no greater than 0.1% (data not shown). Only one such variant fulfilled these criteria, and it mapped to exon 4 of *KCTD7*, which is found in chromosomal region 7q11.21 and encodes potassium channel tetramerization domain-containing protein 7 (isoform 1 [RefSeq accession number NM_153033]; isoform 2 [RefSeq NM_001167961.2]). This *KCTD7* variant—c.550C>T leading to the predicted

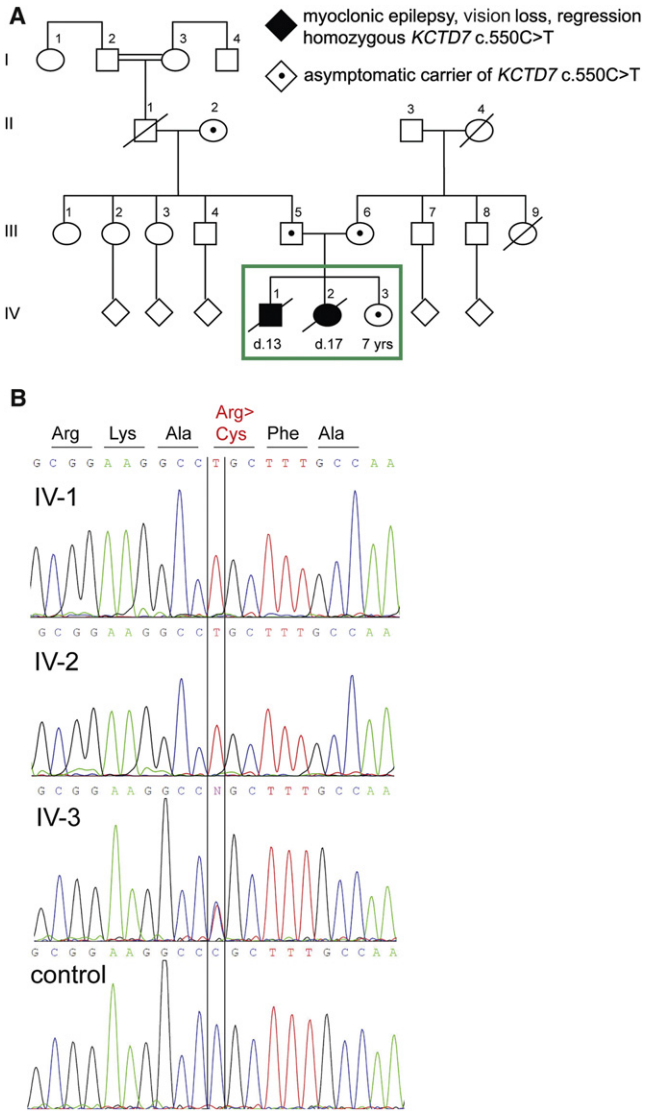

Figure 2. A Private *KCTD7* Variant Identified by Whole-Exome Sequence Analysis of an Affected Sibling Pair and an Unaffected Sibling

(A) A pedigree of the family shows similarly affected siblings (IV-1 and IV-2) that were ruled out for known forms of NCL by enzymatic and molecular testing. I-2 and I-3 are second cousins. Although no known consanguinity existed between the parents of the affected sibling pair, both sides of the family originate from neighboring villages in the state of Michoacán, Mexico. The green box indicates the sibling trio analyzed by whole-exome sequencing.

(B) Sanger-sequence confirmation of the c.550C>T variant in exon 4 of *KCTD7*.

missense change p.Arg184Cys—was confirmed by Sanger sequencing and was found to cosegregate in a recessive pattern with the clinical phenotype; both affected siblings were homozygous for the change, and the unaffected sibling (IV-3), both parents (III-5, III-6), and paternal grandmother (II-2) were heterozygous for the variant (Figures 2A and 2B). The c.550C>T variant in *KCTD7* was also absent in another 822 control individuals from the 1000 Genomes Project;[8] 58 of these controls were of Mexican ancestry. Moreover, the p.Arg184Cys missense change was predicted to be deleterious by HumVar-trained PolyPhen-2[9] and SIFT[10] and is found in a particularly highly conserved region of KCTD7 (Figure S1, available online).

Mutations in *KCTD7* have previously been linked to progressive myoclonic epilepsy (PME) in two families (Table 1).[11,12] Similar to the subjects we describe here, affected members of these families presented before 2 years of age with myoclonic seizures primarily affecting the face and extremities. All affected individuals showed developmental regression, and their disease progressed to death or severe disability by the first or second decade of life. Given that PME is one of several seizure types observed in NCL and given the strong evidence that the p.Arg184Cys *KCTD7* mutation is the causal variant in the NCL-affected family studied here, we performed Sanger sequencing of the *KCTD7* coding region on an additional set of 32 NCL samples (comprising both recessive and dominant forms of NCL with heterogeneous seizure types) that remain without molecular diagnosis. However, no further *KCTD7* mutations were identified in this collection of samples.

In the Van Bogaert et al. study, in which a homozygous KCTD7 nonsense change (p.Arg99*) was found in three PME subjects in a large consanguineous Moroccan family, the ultrastructural analysis of skin biopsies from two of the affected individuals was reported to be normal, implying that there was no lysosomal storage in this family.[11] Whether other PME subjects with *KCTD7* mutations were evaluated for lysosomal storage was not evident (Table 1). Therefore, it is unclear whether *KCTD7* mutations produce allele-specific forms of PME, with or without lysosomal storage, or whether these cases in fact represent forms of NCL with false-negative peripheral biopsy results; this latter scenario has been reported to be problematic in the diagnosis of other forms of NCL.[13] Of note, allele-specific subphenotypes within the NCLs have also been described. For example, the homozygous c.70C>G mutation in *CLN8* produces northern epilepsy (progressive epilepsy with mental retardation), which is an early-onset form of NCL without vision loss[14] and is distinct from variant late-infantile forms of CLN8 associated with vision loss. Similarly, certain mutations in *CLN6* cause adult-onset forms of NCL without vision loss and appear to be mutually exclusive with those that cause variant late-infantile NCL with vision loss.[15]

KCTD7 bears an N-terminal *b*ric à brac, *t*ramtrack, and *b*road complex/*po*xvirus *z*inc finger (BTB/POZ) domain that is homologous to the T1 tetramerization domain of voltage-gated potassium channels[16] and is shared with several other functionally diverse members of the *K*+ *c*hannel *t*etramerization *d*omain, or KCTD, protein family.[17–20] Little is known about the in vivo function of KCTD7, but *Kctd7* transcripts are highly expressed throughout the murine brain, particularly in the mitral cells of the olfactory bulb, hippocampus, cerebral cortex,

Table 1. Clinicopathologic Comparison of Individuals with *KCTD7* Mutations

	Individuals with *KCTD7* Mutations					
	IV-1 (This Study)	**IV-2 (This Study)**	**Subject 1[11]**	**Subject 2[11]**	**Subject 3[11]**	**Subject 4[12]**
Age of onset	9 months	8 months	18 months	24 months	16 months	10 months
Sex	male	female	female	female	female	male
Ethnicity	Mexican	Mexican	Moroccan	Moroccan	Moroccan	Turkish
KCTD7 mutation	c.550C>T (p.Arg184Cys)	c.550C>T (p.Arg184Cys)	c.295C>T (p.Arg99*)	c.295C>T (p.Arg99*)	c.295C>T (p.Arg99*)	c.280C>T (p.Arg94Trp)
Presenting symptoms	myoclonus (face and extremities) and spasticity	myoclonus (face and extremities) precipitated by fevers	myoclonus (face and extremities)	tonic-clonic seizures and myoclonus precipitated by fevers	myoclonus (extremities), head shaking, sudden loss of tone with brief absences	myoclonic seizures, tonic episodes, hypotonia, dystonia, and dyskinesia
Developmental regression	yes	yes	yes	yes	yes	yes
Eye findings	vision loss (normal retinal exam)	vision loss with mild optic atrophy	NR	NR	normal vision	NR
Brain imaging (age)	cerebellar cortical atrophy and thinning of the corpus callosum with loss of subcortical white matter (12 years)	moderate generalized brain atrophy more pronounced in the frontal lobes and cerebellum (13 years)	NR	NR	normal (19 months)	NR
Lysosomal storage	ND	NCL-type storage in buffy coat and skin	absent	NR	absent	NR
Disease course	disease progression and death at 13 years	disease progression, status epilepticus, and death at 17 years	disease progression and wheel-chair bound by 9 years	severe intellectual disability, microcephaly, and seizure free on medication	disease progression, severe ataxia, worsening seizures, and death from sepsis at 3 years	seizures resistant to treatment

The following abbreviations are used: NR, not reported; ND, not determined; and NCL, neuronal ceroid lipofuscinosis.

and Purkinje neurons of the cerebellum.[21] Overexpression of *KCTD7* was reported to decrease the excitability of cultured murine embryonic cortical neurons,[21] but whether this effect was mediated through potassium or other ion channels was unclear.

To further investigate endogenous KCTD7 in the mouse, we harvested multiple organs from a wild-type 5-month-old C57BL/6J mouse, and we extracted proteins with Tris-buffered saline containing 0.2% Triton X-100. Immunoblotting for KCTD7 with a rabbit polyclonal antibody (ab83237 from Abcam [Cambridge, MA]) recognizing the N-terminus of the protein revealed in whole-brain tissue a high expression of a major ~31 kDa form that comigrated with full-length KCTD7 that resulted from transient *KCTD7* overexpression in HEK 293T cells (Figure 3A). Other major immunoreactive bands included a ~28 kDa species, which was particularly prominent in the spleen, liver, and kidneys, a ~37 kDa species most evident in the kidneys, and a ~62 kDa form most likely corresponding to an SDS-stable dimer, which we also observed in the *KCTD7*-transiently-transfected HEK 293T cells, but not in untransfected HEK 293T cells (Figure 3A and Figure S2A). Evidence for KCTD7 homodimerization was also previously reported by Azizieh et al., who found that differently tagged forms of KCTD7 in COS7 cells coimmunoprecipitated.[21] The specificity of the bands was assessed by secondary-only immunoblots, which yielded no bands (data not shown), and by immunoblotting with two additional commercially available KCTD7 antibodies, which also labeled the above-described bands and gave no signal when they were preincubated with the peptide antigen (Figure S2). Here, the presence of multiple immunoreactive bands is consistent with evidence of alternative splice variants[21] and might indicate proteolytic cleavage products. Therefore, despite the apparent ubiquitous expression of *KCTD7* as assessed by Northern blotting,[21] these data strongly suggest tissue-specific differences in KCTD7 regulation.

Given the high expression of *Kctd7* in brain tissue, including in cerebellar granule cells and Purkinje neurons (Allen Brain Atlas), and the prominent cerebellar pathology observed in patients, we assessed KCTD7 levels and localization in conditionally immortalized murine cerebellar granule cells, which have previously been extensively used for cell biological studies of NCL.[22] Of the species detected on immunoblots of whole-tissue homogenates, the ~28 kDa form was the most prominent. Interestingly, all species, i.e., ~28 kDa, ~31 kDa, and ~62 kDa isoforms, were significantly elevated in cerebellar granule cells derived from a murine JNCL model (Cb*Cln3*$^{\Delta ex7/8/\Delta ex7/8}$)[21] (Figure 3A). This suggested an impact of CLN3 loss of function on KCTD7 turnover

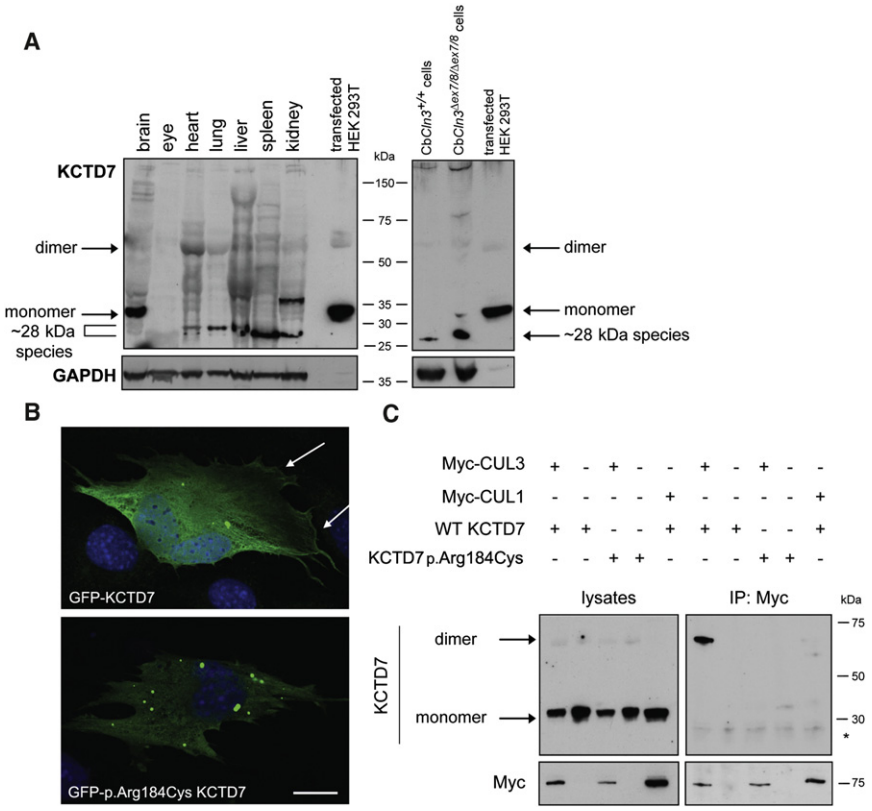

Figure 3. KCTD7 Is Abundant in Brain Tissue, and the NCL-Associated Variant Alters Its Subcellular Localization and Disrupts Its Interaction with Cullin-3

(A) The left panel shows protein lysates that were isolated from the indicated tissues from a wild-type 5-month-old C57BL/6J mouse and then subjected to SDS-PAGE and immunoblotting for KCTD7. Approximately 100 μg of protein were loaded per lane. Five micrograms of protein lysate from HEK 293T cells transfected with wild-type *KCTD7* was loaded as a reference. In the right panel, 30 μg of protein from conditionally immortalized Cb*Cln3*$^{+/+}$ or Cb*Cln3* $^{\Delta ex7/8/\Delta ex7/8}$ murine cerebellar cell lysates was probed for KCTD7 and GAPDH.

(B) Murine cerebellar cells (Cb*Cln3*$^{+/+}$ cells) were transiently transfected with GFP alone (not shown) or with constructs encoding an N-terminal GFP fusion of wild-type or p.Arg184Cys KCTD7, and they were visualized by confocal microscopy. Arrows show sites of plasma-membrane localization. The scale bar represents 15 μm.

(C) HEK 293T cells were transiently transfected with Myc-tagged cullin-3 (CUL3) or cullin-1 (CUL1) and untagged wild-type or p.Arg184Cys KCTD7. Lysates were immunoprecipitated with the Myc antibody and immunoblotted for KCTD7 or Myc. Lysates represent approximately 20% input. The asterisk indicates the immunoglobulin light chain.

because compared with *Kctd7* expression in cells derived from wild-type (Cb*Cln3*$^{+/+}$) littermates,[23] *Kctd7* expression in Cb*Cln3*$^{\Delta ex7/8/\Delta ex7/8}$ cerebellar cells was essentially unchanged. Because immunohistochemistry did not successfully detect KCTD7, we generated N-terminal green fluorescent protein (GFP)-tagged forms of wild-type and p.Arg184Cys KCTD7 by using Gateway Technology (Invitrogen, Carlsbad, CA) and transiently transfected cerebellar cells with the TransIt Express reagent (Mirus Technologies, Madison, WI) (Figure 3B and Figures S2 and S3) in order to assess whether the identified mutation affected expression and/or localization. Wild-type GFP-KCTD7 showed broad, somewhat punctate cytoplasmic localization and distinct signal at the plasma membrane. In contrast, GFP-KCTD7 p.Arg184Cys showed more diffuse cytoplasmic localization and markedly diminished plasma-membrane signal, as well as prominent cytoplasmic aggregates (Figure 3B and Figure S3). All together, these results suggest that the mutation affects the trafficking and/or solubility of KCTD7. Expression of GFP alone or of another fusion protein, GFP-LC3, a marker of autophagosomes,[24] did not produce similar aggregates in cerebellar cells (data not shown and Cao et al.[25]). Additional localization studies in other neuronal subtypes, for example, in primary neurons, will help further clarify the impact of the p.Arg184Cys missense change on KCTD7 trafficking, turnover, and function.

Similar to other members of the KCTD family,[17,18] KCTD7 has been shown to interact with Cullin-3,[21] a scaffolding component of several E3 ubiquitin-ligase complexes that selectively tag proteins for degradation by the proteasome.[26] These interactions are mediated, at least in part, through the BTB/POZ domain,[17,18,27] but evidence points to the role of critical residues outside this domain as well.[17,28,29] To determine whether the p.Arg184Cys variant, which falls outside the BTB/POZ domain (Figure S1), affects its interaction with Cullin-3, we transiently cotransfected HEK 293T cells with constructs encoding Myc-tagged Cullin-3 or Cullin-1 (another E3 ubiquitin-ligase protein component) and untagged wild-type or p.Arg184Cys KCTD7, and we immunoprecipitated lysates with a Myc antibody (clone 9E10, Origene, Rockland, MD). Cullin-3, but not Cullin-1, interacted robustly with the SDS-stable dimeric form of wild-type KCTD7, but the p.Arg184Cys missense change abrogated the interaction with Cullin-3 (Figure 3C). The abrogated interaction between KCTD7 and Cullin-3 might lead to an accumulation of substrate proteins, which might be toxic and might lead to altered homeostasis of the ubiquitin-proteasome system (UPS) and the other protein-degradation systems within the cell.

The identification of the *KCTD7* mutation described in this family establishes a rare, infantile-onset subtype of NCL and indicates that *KCTD7* should be considered in

the diagnostic workup for molecularly undefined forms of NCL in addition to PME.[11,12] Moreover, further assessment for evidence of lysosomal storage in PME subjects with *KCTD7* mutations is warranted. In light of our recent findings, we propose a designation of CLN14 for this form of NCL; the synonymous *CLN14* gene symbol for *KCTD7* was approved by the Human Genome Organization (HUGO) Gene Nomenclature Committee. The functional effects of the causal variant in the current study are consistent with the previously defined role of defective protein processing in NCL[25,30] and support a contribution from the UPS. In particular, increasing evidence shows significant crosstalk between autophagy and the UPS in a broad range of neurodegenerative diseases.[31,32] The activity of cullin family members has specifically been linked to endosomal[33] and autophagosomal[34,35] maturation, processes that are defective in a murine model of JNCL.[25] Therefore, determining the substrate(s) of the predicted KCTD7- and Cullin-3-containing ubiquitin-ligase complex and their potential role in NCL pathogenesis will be of great interest in future studies.

Supplemental Data

Supplemental Data include three figures and can be found with this article online at http://www.cell.com/AJHG.

Acknowledgments

This work was supported by the National Institutes of Health National Institute of Neurological Disorders and Stroke (R01NS073813 to S.L.C and R01NS33648 to M.E.M.) and the Batten Disease Support and Research Association (J.F.S.). J.F.S. is supported by a Massachusetts General Hospital Executive Committee on Research Tosteson Award. A.K. receives training support from the Kirschstein National Research Service Award Training Program T32 (grant GM007748-32). We would like to thank the National Heart, Lung, and Blood Institute Grand Opportunity (GO) Exome Sequencing Project and the following ongoing studies, which produced and provided exome variant calls for comparison: the Lung GO Sequencing Project (HL-102923), the Women's Health Initiative Sequencing Project (HL-102924), the Broad GO Sequencing Project (HL-102925), the Seattle GO Sequencing Project (HL-102926), and the Heart GO Sequencing Project (HL-103010). Plasmids encoding Myc-Cullin-1 and Myc-Cullin-3 were gifts from Yue Xiong (plasmids 19896 and 19893, respectively; Addgene, Cambridge, MA). We thank Xin Feng and Yi Cao for expert technical support. S.L.C. and K.B.S. are members of the Batten Disease Support and Research Association scientific and medical advisory boards, respectively.

Received: March 9, 2012
Revised: April 18, 2012
Accepted: May 29, 2012
Published online: June 28, 2012

Web Resources

The URLs for data presented herein are as follows:

Allen Brain Atlas, http://mouse.brain-map.org/
Clustal Omega, http://www.clustal.org/omega
HUGO Gene Nomenclature Committee, http://www.genenames.org/
NCBI UniGene, http://www.ncbi.nlm.nih.gov/unigene/
NCL Mutation Database, http://www.ucl.ac.uk/ncl/mutation.shtml
NHLBI Exome Sequencing Project, http://evs.gs.washington.edu/EVS/
Online Mendelian Inheritance in Man, http://www.omim.org/
PolyPhen-2, http://genetics.bwh.harvard.edu/pph2
SIFT, http://sift.jcvi.org/

References

1. Jalanko, A., and Braulke, T. (2009). Neuronal ceroid lipofuscinoses. Biochim. Biophys. Acta *1793*, 697–709.
2. Kousi, M., Lehesjoki, A.E., and Mole, S.E. (2012). Update of the mutation spectrum and clinical correlations of over 360 mutations in eight genes that underlie the neuronal ceroid lipofuscinoses. Hum. Mutat. *33*, 42–63.
3. Benitez, B.A., Alvarado, D., Cai, Y., Mayo, K., Chakraverty, S., Norton, J., Morris, J.C., Sands, M.S., Goate, A., and Cruchaga, C. (2011). Exome-sequencing confirms DNAJC5 mutations as cause of adult neuronal ceroid-lipofuscinosis. PLoS ONE *6*, e26741.
4. Nosková, L., Stránecký, V., Hartmannová, H., Přistoupilová, A., Barešová, V., Ivánek, R., Hůlková, H., Jahnová, H., van der Zee, J., Staropoli, J.F., et al. (2011). Mutations in DNAJC5, encoding cysteine-string protein alpha, cause autosomal-dominant adult-onset neuronal ceroid lipofuscinosis. Am. J. Hum. Genet. *89*, 241–252.
5. Cooper, J.D. (2010). The neuronal ceroid lipofuscinoses: The same, but different? Biochem. Soc. Trans. *38*, 1448–1452.
6. Li, H., and Durbin, R. (2009). Fast and accurate short read alignment with Burrows-Wheeler transform. Bioinformatics *25*, 1754–1760.
7. McKenna, A., Hanna, M., Banks, E., Sivachenko, A., Cibulskis, K., Kernytsky, A., Garimella, K., Altshuler, D., Gabriel, S., Daly, M., and DePristo, M.A. (2010). The Genome Analysis Toolkit: A MapReduce framework for analyzing next-generation DNA sequencing data. Genome Res. *20*, 1297–1303.
8. Marth, G.T., Yu, F., Indap, A.R., Garimella, K., Gravel, S., Leong, W.F., Tyler-Smith, C., Bainbridge, M., Blackwell, T., Zheng-Bradley, X., et al; 1000 Genomes Project. (2011). The functional spectrum of low-frequency coding variation. Genome Biol. *12*, R84.
9. Adzhubei, I.A., Schmidt, S., Peshkin, L., Ramensky, V.E., Gerasimova, A., Bork, P., Kondrashov, A.S., and Sunyaev, S.R. (2010). A method and server for predicting damaging missense mutations. Nat. Methods *7*, 248–249.
10. Ng, P.C., and Henikoff, S. (2002). Accounting for human polymorphisms predicted to affect protein function. Genome Res. *12*, 436–446.
11. Van Bogaert, P., Azizieh, R., Désir, J., Aeby, A., De Meirleir, L., Laes, J.F., Christiaens, F., and Abramowicz, M.J. (2007). Mutation of a potassium channel-related gene in progressive myoclonic epilepsy. Ann. Neurol. *61*, 579–586.
12. Krabichler, B., Rostasy, K., Baumann, M., Karall, D., Scholl-Bürgi, S., Schwarzer, C., Gautsch, K., Spreiz, A., Kotzot, D., Zschocke, J., et al. (2012). Novel Mutation in Potassium Channel related Gene KCTD7 and Progressive Myoclonic Epilepsy. Ann. Hum. Genet. *76*, 326–331.

13. Sadzot, B., Reznik, M., Arrese-Estrada, J.E., and Franck, G. (2000). Familial Kufs' disease presenting as a progressive myoclonic epilepsy. J. Neurol. *247*, 447–454.
14. Wisniewski, K.E., Zhong, N., and Philippart, M. (2001). Pheno/genotypic correlations of neuronal ceroid lipofuscinoses. Neurology *57*, 576–581.
15. Arsov, T., Smith, K.R., Damiano, J., Franceschetti, S., Canafoglia, L., Bromhead, C.J., Andermann, E., Vears, D.F., Cossette, P., Rajagopalan, S., et al. (2011). Kufs disease, the major adult form of neuronal ceroid lipofuscinosis, caused by mutations in CLN6. Am. J. Hum. Genet. *88*, 566–573.
16. Benatar, M. (2000). Neurological potassium channelopathies. QJM *93*, 787–797.
17. Bayón, Y., Trinidad, A.G., de la Puerta, M.L., Del Carmen Rodríguez, M., Bogetz, J., Rojas, A., De Pereda, J.M., Rahmouni, S., Williams, S., Matsuzawa, S., et al. (2008). KCTD5, a putative substrate adaptor for cullin3 ubiquitin ligases. FEBS J. *275*, 3900–3910.
18. Correale, S., Pirone, L., Di Marcotullio, L., De Smaele, E., Greco, A., Mazzà, D., Moretti, M., Alterio, V., Vitagliano, L., Di Gaetano, S., et al. (2011). Molecular organization of the cullin E3 ligase adaptor KCTD11. Biochimie *93*, 715–724.
19. Metz, M., Gassmann, M., Fakler, B., Schaeren-Wiemers, N., and Bettler, B. (2011). Distribution of the auxiliary GABAB receptor subunits KCTD8, 12, 12b, and 16 in the mouse brain. J. Comp. Neurol. *519*, 1435–1454.
20. Schwenk, J., Metz, M., Zolles, G., Turecek, R., Fritzius, T., Bildl, W., Tarusawa, E., Kulik, A., Unger, A., Ivankova, K., et al. (2010). Native GABA(B) receptors are heteromultimers with a family of auxiliary subunits. Nature *465*, 231–235.
21. Azizieh, R., Orduz, D., Van Bogaert, P., Bouschet, T., Rodriguez, W., Schiffmann, S.N., Pirson, I., and Abramowicz, M.J. (2011). Progressive myoclonic epilepsy-associated gene KCTD7 is a regulator of potassium conductance in neurons. Mol. Neurobiol. *44*, 111–121.
22. Fossale, E., Wolf, P., Espinola, J.A., Lubicz-Nawrocka, T., Teed, A.M., Gao, H., Rigamonti, D., Cattaneo, E., MacDonald, M.E., and Cotman, S.L. (2004). Membrane trafficking and mitochondrial abnormalities precede subunit c deposition in a cerebellar cell model of juvenile neuronal ceroid lipofuscinosis. BMC Neurosci. *5*, 57.
23. Cao, Y., Staropoli, J.F., Biswas, S., Espinola, J.A., MacDonald, M.E., Lee, J.M., and Cotman, S.L. (2011). Distinct early molecular responses to mutations causing vLINCL and JNCL presage ATP synthase subunit C accumulation in cerebellar cells. PLoS ONE *6*, e17118.
24. Tanida, I. (2011). Autophagy basics. Microbiol. Immunol. *55*, 1–11.
25. Cao, Y., Espinola, J.A., Fossale, E., Massey, A.C., Cuervo, A.M., MacDonald, M.E., and Cotman, S.L. (2006). Autophagy is disrupted in a knock-in mouse model of juvenile neuronal ceroid lipofuscinosis. J. Biol. Chem. *281*, 20483–20493.
26. Willems, A.R., Schwab, M., and Tyers, M. (2004). A hitchhiker's guide to the cullin ubiquitin ligases: SCF and its kin. Biochim. Biophys. Acta *1695*, 133–170.
27. Pintard, L., Willems, A., and Peter, M. (2004). Cullin-based ubiquitin ligases: Cul3-BTB complexes join the family. EMBO J. *23*, 1681–1687.
28. Figueroa, P., Gusmaroli, G., Serino, G., Habashi, J., Ma, L., Shen, Y., Feng, S., Bostick, M., Callis, J., Hellmann, H., and Deng, X.W. (2005). Arabidopsis has two redundant Cullin3 proteins that are essential for embryo development and that interact with RBX1 and BTB proteins to form multisubunit E3 ubiquitin ligase complexes in vivo. Plant Cell *17*, 1180–1195.
29. Kwon, J.E., La, M., Oh, K.H., Oh, Y.M., Kim, G.R., Seol, J.H., Baek, S.H., Chiba, T., Tanaka, K., Bang, O.S., et al. (2006). BTB domain-containing speckle-type POZ protein (SPOP) serves as an adaptor of Daxx for ubiquitination by Cul3-based ubiquitin ligase. J. Biol. Chem. *281*, 12664–12672.
30. Oresic, K., Mueller, B., and Tortorella, D. (2009). Cln6 mutants associated with neuronal ceroid lipofuscinosis are degraded in a proteasome-dependent manner. Biosci. Rep. *29*, 173–181.
31. Cherra, S.J., 3rd, Dagda, R.K., and Chu, C.T. (2010). Review: Autophagy and neurodegeneration: survival at a cost? Neuropathol. Appl. Neurobiol. *36*, 125–132.
32. Santos, R.X., Cardoso, S., Correia, S., Carvalho, C., Santos, M.S., and Moreira, P.I. (2010). Targeting autophagy in the brain: A promising approach? Cent. Nerv. Syst. Agents Med. Chem. *10*, 158–168.
33. Huotari, J., Meyer-Schaller, N., Hubner, M., Stauffer, S., Katheder, N., Horvath, P., Mancini, R., Helenius, A., and Peter, M. (2012). Cullin-3 regulates late endosome maturation. Proc. Natl. Acad. Sci. USA *109*, 823–828.
34. Pearce, C., Hayden, R.E., Bunce, C.M., and Khanim, F.L. (2009). Analysis of the role of COP9 Signalosome (CSN) subunits in K562; the first link between CSN and autophagy. BMC Cell Biol. *10*, 31.
35. Su, H., Li, F., Ranek, M.J., Wei, N., and Wang, X. (2011). COP9 signalosome regulates autophagosome maturation. Circulation *124*, 2117–2128.